

## CHRONOPOTENTIOMETRIC STUDY OF EC MECHANISM DURING THE FIRST CYCLE OF ALTERNATING CURRENT

Angela MOLINA<sup>1</sup>, Francisco MARTINEZ-ORTIZ<sup>2</sup>, Ricardo RUIZ  
and Manuela LOPEZ-TENES<sup>3</sup>

*Departamento de Química Física, Universidad de Murcia, Espinardo 30071 Murcia, Spain;*  
*e-mail: <sup>1</sup>amolina@fcu.um.es, <sup>2</sup>fmortiz@fcu.um.es, <sup>3</sup>manuela@fcu.um.es*

Received June 21, 1996

Accepted December 8, 1996

The theoretical approach to the application of the first period of a sinusoidal current at static and dynamic spherical electrodes for study of EC mechanism is presented. Methods for determining heterogeneous and homogeneous kinetic parameters are proposed. In order to check theoretical result, the rate of benzidine rearrangement was evaluated from transition time measurements.

**Key words:** First period; Benzidine rearrangement; Heterogeneous kinetic parameters; Homogeneous kinetic parameters.

In a previous paper we have carried out a general study of the CE and EC mechanisms using chronopotentiometry with various current–time functions at usual types of electrodes<sup>1</sup>. These techniques, in which current does not change the sign during the experiment, are useful for determination of kinetic parameters of chemical reactions preceding the charge transfer reaction from transition times. However, when chemical steps follow charge transfer reactions, kinetic information cannot be obtained from the transition time but only from the complete potential–time curve. Therefore, the calculation of chemical kinetic parameters is more difficult and is affected by the kinetics of the charge transfer reaction<sup>2–6</sup>. For those cases, perturbations in which the sign of the current changes (alternating current) are more adequate. The kinetic information of the chemical step can be obtained from transition times of the oxidation process, achieved after the first change of the current sign.

In refs<sup>7–9</sup> we have analyzed the application of an alternating current of low frequency and large amplitude to different types of electrodes to study a simple charge transfer reaction. We have shown the advantages of these procedures for determination of heterogeneous kinetic parameters  $\alpha$  and  $k_s$ . The potential–time curves obtained with this technique are little affected by the charging of the double layer, however, the effects of electrode curvature are enhanced.

In this work we have developed a rigorous theory describing the response of EC mechanism to the alternating current of the form  $I(t) = I_0 \sin \omega t$  applied to a DME. It is

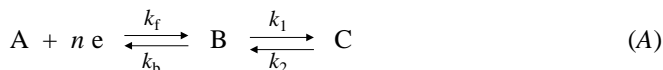
using a more rigorous model of an expanding sphere and assuming, for convenience, the existence of a blank period  $t_1 \geq 0$ . We have also considered an asymptotic solution applicable when the steady state is reached in the reaction layer. From the equations deduced in this paper for the dropping mercury electrode (DME), the response corresponding to a static mercury dropping electrode (SMDE) and to a static plane electrode can be obtained as particular cases.

In spite of the equations obtained in this paper being valid for any number of cycles of the alternating current, only the first cycle appears to be the most interesting for the study of EC mechanism. Moreover, the alternating current is applied under conditions in which the direct transition time,  $\tau_A$ , is not reached. In this case, when only species A is initially present in solution, the transition time corresponding to the oxidation process always exists and only depends on chemical kinetics but not on most of the experimental parameters (electrode area, alternating current amplitude, *etc.*). Owing to this characteristic, the diagnosis of an EC mechanism is immediate, and its quantitative characterization is very easy. Consequently, this technique can be advantageous compared to more popular potentiostatic techniques. We have proposed methods for calculation of equilibrium and rate constants of the chemical reaction following charge transfer reaction and also for determining the kinetic parameters of the charge transfer reaction.

Finally, we have applied the methods described in this paper to the extensively studied reaction of benzidine rearrangement which has been the reference for most of the theoretical electrochemical studies on the EC mechanism<sup>10-14</sup>. Our results are in a good agreement with those previously reported.

## THEORETICAL

The EC mechanism is described by the Eq. (A).



The corresponding boundary value problem is given by (see Symbols for notation)

$$\hat{\delta}_A C_A = 0 \quad (1)$$

$$\hat{\delta}_B C_B = -\hat{\delta}_C C_C = -k_1 C_B + k_2 C_C \quad (2)$$

$$\left. \begin{array}{l} t = 0, r \geq r_0 \\ t > 0, r \rightarrow \infty \end{array} \right\} C_A = C_A^*, C_B = C_B^*, C_C = C_C^* \quad (3)$$

$$K = \frac{C_B^*}{C_C^*} = \frac{k_2}{k_1} \quad (4)$$

$t > 0, r = r_0$

$$D_A \left( \frac{\partial C_A}{\partial r} \right)_{r=r_0} = -D_B \left( \frac{\partial C_B}{\partial r} \right)_{r=r_0} = \frac{I(t)}{nFA(t_s)} \quad (5)$$

$$D_C \left( \frac{\partial C_C}{\partial r} \right)_{r=r_0} = 0 \quad (6)$$

Moreover,

$$\frac{I(t)}{nFA(t_s)} = k_f C_A(r_0, t) - k_b C_B(r_0, t) \quad (7)$$

where  $\hat{\delta}_i$  is the operator corresponding to the expanding sphere<sup>15</sup>

$$\hat{\delta}_i = \frac{\partial}{\partial t} - D_i \left( \frac{\partial^2}{\partial r^2} + \frac{2}{r} \frac{\partial}{\partial r} \right) + \frac{a^3}{3r^2} \frac{\partial}{\partial r} \quad (8)$$

In the following, we assume that

$$D_A \neq D_B = D_C \quad (9)$$

When an alternating current of the form

$$I(t) = I_0 \sin \Omega t \quad (10)$$

is applied to a DME with  $\Omega = \omega t$  (Eq. (A6)), by a procedure similar to that described in refs.<sup>1,7,8</sup>, we deduce for the surface concentrations of A and B species (see Appendix),

$$\frac{C_A(r_0, t)}{C_A^*} = 1 - N_{\text{DME}} t^{1/2} S_A \quad (11)$$

$$\frac{C_B(r_0, t)}{C_A^*} = \frac{1}{1 + K} \{ K \mu_{EC} + \gamma N_{DME} t^{1/2} [K S_B + X_B] \}, \quad (12)$$

where

$$N_{DME} = \frac{2I_0}{nFA(t_s) \sqrt{D_A C_A^*}} \quad (13)$$

$$A(t_s) = A_0 t_s^{2/3} \quad (14)$$

$$t_s = t_1 + t \quad (15)$$

$$\mu_{EC} = \frac{C_B^* + C_C^*}{C_A^*} \quad (16)$$

$$\gamma = \left( \frac{D_A}{D_B} \right)^{1/2}. \quad (17)$$

$t_1$  is a blank period elapsed between the time when the drop is breaking off and the application of the current and  $t$  is the time elapsed between the application of the current and the measurement of the potential.  $S_i$  ( $i = A$  or  $B$ ) and  $X_B$  are functional series defined in the Appendix. These series are valid for a DME. However, they can be easily transformed for an SMDE and a static plane electrode by simple transformations according to Eqs (A15)–(A19). All general expressions deduced in this paper are therefore applicable to any static or dynamic electrode, spherical or planar.

When  $I_0$  and/or  $\omega$  in Eq. (10) take values such that the transition time of species A,  $\tau_A$ , is reached (before the change of the current sign), the results obtained with a sinusoidal current do not differ substantially from those with a programmed current<sup>1–7</sup>. In this case, when  $t = \tau_A$ , the experiment must be stopped to avoid decomposition of supporting electrolyte. This possibility is not very interesting for the study of an EC process, since  $\tau_A$  is identical to that deduced for an electrochemical process and independent on chemical kinetic parameters as indicated by Eq. (11).

When the depletion of A at the electrode surface does not occur, and when species B and C are not initially present in the solution, the transition time of B,  $\tau_B$ , is always reached (after the first change of the alternating current sign). However, if species B and C are initially present in the solution,  $\tau_B$  may or may not be reached depending on the value of  $C_B^* + C_C^*$  (ref.<sup>8</sup>). The general expression for  $\tau_B$  is deduced by setting  $C_B(r_0, t)$  in Eq. (12) equal to zero, so we obtain

$$\tau_B^{1/2} = \frac{-KnFA_0(t_1 + \tau_B)^{2/3}\sqrt{D_B}(C_B^* + C_C^*)}{2I_0 [KS_B + X_B]_{t=\tau_B}} \quad (18)$$

For  $C_B^* + C_C^* = 0$ , the equation is simplified to

$$[KS_B + X_B]_{t=\tau_B} = 0 \quad (19)$$

The transition time  $\tau_B$ , corresponding to the oxidation of species B is function of the rate constants of the chemical reaction since  $\chi = (k_1 + k_2)t$  (series  $X_B$  in Eq. (A10)). Thus, it is possible to determine  $k_1$  and  $k_2$  from measurements of  $\tau_B$  (see Results).

From Eq. (19) it is clear that, when only species A is initially present in the solution,  $\tau_B$  is independent of most of the experimental conditions, such as  $I_0$ ,  $C_A^*$ , electrode area, etc.

The general potential–time response can be deduced by introducing Eqs (11) and (12) into Eq. (7)

$$\frac{N_{DME}\sqrt{D_A}}{2k_s} \sin(\Omega) e^{\alpha\eta(t)} = 1 - N_{DME} t^{1/2} S_A - \frac{e^{\eta(t)}}{1+K} \{K\mu_{EC} + \gamma N_{DME} t^{1/2} [KS_B + X_B]\}, \quad (20)$$

where

$$\eta(t) = \frac{nF}{RT} [E(t) - E^0] \quad (21)$$

For a reversible process ( $k_s \rightarrow \infty$ ), when  $\mu_{EC} = 0$ , Eq. (20) becomes

$$E(t) = E^0 + \frac{RT}{nF} \ln \frac{(1+K)}{\gamma N_{DME}} + \frac{RT}{nF} \ln \frac{1 - N_{DME} t^{1/2} S_A}{t^{1/2} (KS_B + X_B)} \quad (22)$$

For totally irreversible process ( $k_s \ll 1 \text{ cm}^{-1}$ ) two following situations are possible:

a) For  $I(t) > 0$  ( $\omega t < \pi$ ) Eq. (20) takes the form

$$\left. \begin{aligned} E(t) &= E^0 + \frac{RT}{\alpha nF} \ln \frac{2k_s}{N_{DME}\sqrt{D_A}} + \frac{RT}{\alpha nF} \ln g_c \\ g_c &= \frac{1 - N_{DME} t^{1/2} S_A}{\sin \Omega} \end{aligned} \right\} \quad (23)$$

b) For  $I(t) < 0$  ( $\pi < \omega t < 2\pi$ ) Eq. (20) is transformed into

$$\left. \begin{aligned} E(t) &= E^0 - \frac{RT}{(1-\alpha)nF} \ln \frac{2k_s}{N_{\text{DME}}\sqrt{D_A}} + \frac{RT}{(1-\alpha)nF} \ln g_a \\ g_a &= \frac{-(1+K) \sin \Omega}{N_{\text{DME}}\gamma^{1/2}[KS_B + X_B]} \end{aligned} \right\} \quad (24)$$

As can be deduced from Eqs (23) and (24), the potential–time response for the cathodic current  $I(t) > 0$ , given by Eq. (10), is independent on the kinetic parameters of the chemical step and it does not differ from that obtained for a simple, irreversible charge transfer process. On the other hand, the potential–time response associated with anodic current  $I(t) < 0$  is affected by the presence of the chemical reaction and depends both on  $K$  and  $k$  ( $k = k_1 + k_2$ ) as follows from series  $X_B$ , Eq. (A10). This behaviour will be analyzed below.

## THEORETICAL RESULTS

### Surface Concentrations and Transition Times

The expressions for the surface concentrations corresponding to an EC process, Eqs (11), (12) and, therefore, potential–time response depend on the series  $S_A$ ,  $S_B$  and  $X_B$  given by Eqs (A1) and (A10). The series  $S_i$  ( $i = A$  or  $B$ ) corresponds to the electrochemical process, and, therefore, has diffusive character. The surface concentration of A according to Eq. (11) does not differ from that obtained for electrochemical mechanism. On the other hand, series  $X_B$ , which appears in the expression  $C_B(r_0, t)$ , Eq. (12), depends on the chemical constants  $k_1$  and  $k_2$ , Eq. (A14), and, therefore, on the chemical kinetics. This series decreases with increasing  $\chi$  and has the following lower and upper limits:

$$[X_B(\xi_B, \beta, \chi, \Omega)]_{\chi \rightarrow \infty} \rightarrow 0 \quad (25)$$

$$[X_B(\xi_B, \beta, \chi, \Omega)]_{\chi \rightarrow 0} \rightarrow S_B(\xi_B, \beta, \Omega) \quad (26)$$

Equation (25) can easily be verified by taking into account large values of  $\chi$ , for which the steady-state approximation can be applied. The expression for  $X_B$  is simplified to

$$X_B = \frac{\sin \Omega}{2\chi^{1/2}} \quad \text{for } \chi \geq 20 \quad (27)$$

for any type of electrode (DME, SMDE or planar electrodes).

Moreover, it can easily be proved from Eqs (12), (25)–(27) that the EC mechanism has attributes of a simple electrochemical process in two following cases: considering  $\mu_{EC} = (1 + K)C_B^*/KC_A^*$  for  $\chi \rightarrow 0$ ,  $K > 0$  and for  $K \gg 1$ , any value of  $\chi$ .

Indeed, by substituting one of above mentioned conditions into Eq. (12) we obtain

$$\frac{C_B(r_0, t)}{C_A^*} = \frac{C_B^*}{C_A^*} + \gamma N_{DME} t^{1/2} S_B, \quad (28)$$

which is identical to the equation for electrochemical mechanism<sup>7,8</sup>.

Other subjects of interest are  $\chi \rightarrow \infty$  and  $K > 0$ .

The transition time for an EC mechanism (only species A present in solution) is coincident with that for a charge transfer reaction (E process), as can easily be found by setting  $C_B(r_0, t)$  in Eq. (12) equal to zero (note that under these conditions  $\mu_{EC} = 0$  and  $X_B(\xi_B, \beta, \chi, \Omega) = 0$ ).

In the case of  $K \rightarrow 0$ , Eq. (12) is transformed into

$$\frac{C_B(r_0, t)}{C_A^*} = \gamma N_{DME} t^{1/2} X_B \quad (29)$$

*i.e.* an EC process has now a most pronounced kinetic character.

#### Determination of Kinetic Parameters

For determining the rate constants  $k_1$  and  $k_2$  of the posterior chemical step it is necessary to know the value of the equilibrium constant  $K$ . It can be determined, *e.g.*, by extrapolation of the transient response (potential–time curve) to the equilibrium response (near zero time) as long as species A, B and C are initially present in the solution.

For  $t \rightarrow 0$  in Eq. (20), we obtain

$$E(t \rightarrow 0) - E^0 = \frac{RT}{nF} \ln \frac{(1 + K)}{K\mu_{EC}}. \quad (30)$$

Once  $K$  is known, the rate constants can easily be deduced from the curves plotted in Fig. 1. In this figure we have represented the variation of  $\tau_B/\tau_{B_E}$  vs  $\chi_{t=\tau_B}$ . The experimental conditions ( $I_0$ ,  $C_A^*$  and electrode area) have been chosen in such a way that  $\tau_A$  is not reached and  $\tau_B$  exists. In other words,  $N_{DME} < N_{DME_{min}}$  (see Eq. (39) in ref.<sup>8</sup>). This figure corresponds to the more usual situation for an EC process in which only species A is initially present in solution ( $\mu_{EC} = 0$ ). In this case,  $\tau_B/\tau_{B_E}$  or  $\Omega_{t=\tau_B}/\Omega_{t=\tau_{B_E}}$  and  $\chi_{t=\tau_B}$  are related through the equations

$$[X_B(\xi_B, \beta, \chi, \Omega)]_{t=\tau_B} = -K[S_B(\xi_B, \beta, \Omega)]_{t=\tau_B} \quad (31)$$

and

$$[S_B(\xi_B, \beta, \Omega)]_{t=\tau_{B_E}} = 0 \quad (32)$$

From these curves the determination of  $k_1 + k_2$  for  $K$  values near zero is immediate. For large values of  $K$ , at least two measurements of  $\tau_B$ , corresponding to different  $\omega$  values, must be carried out in order to select the adequate branch of the working curve.

These curves present, among others, the following advantages:

a) it is possible to determine  $k_1$  and  $k_2$  directly from experimental values of  $\tau_B$ .

b) The curves remain valid when the frequency of alternating current  $\omega$  is changed and the electrode sphericity is not taken into account ( $\xi_B = 0$ ) (Fig. 1). This feature is due to the fact that Eqs (31) and (32) depend on  $\omega$  ( $\Omega = \omega t$ ). Therefore, for a plane electrode, the series  $S_B$  ( $\xi_B = 0, \beta, \Omega$ ) and  $X_B$  ( $\xi_B = 0, \beta, \chi, \Omega$ ) depend only on  $\Omega$  and  $\chi$  at  $\Omega_1 = \omega t_1$  fixed since the parameters  $\beta$  and  $\Omega$  are related by

$$\beta = \frac{t}{t_1 + t} = \frac{\Omega}{\Omega_1 + \Omega} \quad (33)$$

and

$$\frac{\tau_B}{\tau_{B_E}} = \frac{\Omega_{t=\tau_B}}{\Omega_{t=\tau_{B_E}}} \quad (34)$$

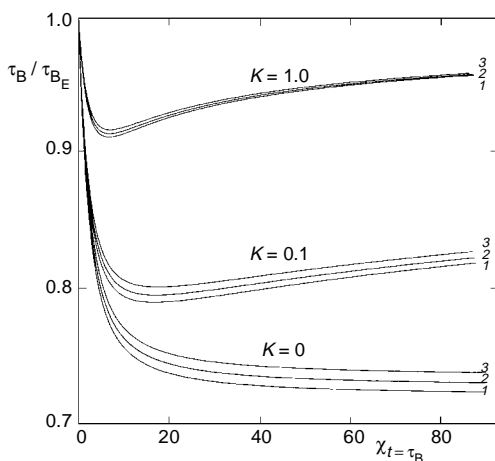


FIG. 1  
Working curves deduced from Eqs (31) and (32) for a DME with the expanding plane electrode model ( $\xi_B = 0$ ) for different values of  $K$ . The values of  $\Omega_1$  are: 1 0, 2 1, 3 3



c) For calculation of  $k_1$  and  $k_2$ ,  $\tau_B$  can be determined fairly reliably, taking into account that when only species A is initially present in the solution (Eq. (28)), then  $\tau_B$  is independent of  $N_{\text{DME}} t_s^{2/3}$ , i.e. of the values of  $I_0$ ,  $C_A^*$ , etc. as follows from Eq. (13).

### Potential–Time Curves

Figure 2 shows the influence of the rate constant  $k_1$  on  $E(t) - E^0$  vs  $t$  plots ( $E-t$  curves), corresponding to an irreversible EC mechanism ( $K = 0$ ) where the electrochemical step is reversible. These curves are shifted to more negative potentials and the transition time increases when  $k_1$  diminishes. In Fig. 3 we have plotted the  $E-t$  curves obtained for different values of  $k = k_1 + k_2$  for  $K > 0$ . In this case it can be noticed that for high and low  $k$  values (curves 1 and 4) the transition times are coincident, since in both cases the EC mechanism behaves as an E process (Eqs (12) and (28)) as discussed

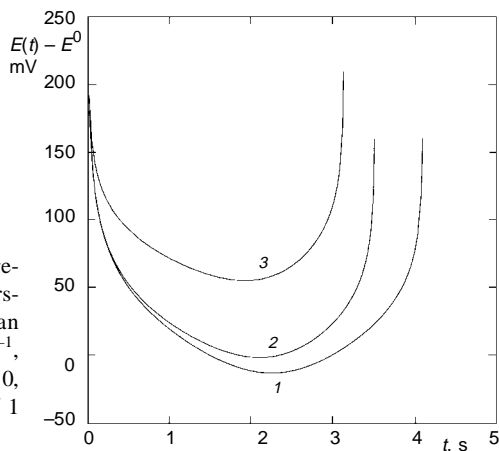


FIG. 2

Potential–time curves at an SMDE corresponding to an EC mechanism with a reversible charge transfer reaction and an irreversible chemical step ( $K = 0$ ),  $\omega = 1 \text{ s}^{-1}$ ,  $N_{\text{SMDE}} = 1 \text{ s}^{-1/2}$ ,  $\xi_{\text{OA}} = \xi_{\text{OB}} = 0.1 \text{ s}^{-1/2}$ ,  $\mu_{\text{EC}} = 0$ ,  $\gamma = 1$ ,  $T = 298 \text{ K}$ . The values of  $k_1$  ( $\text{s}^{-1}$ ) are: 1  $1 \cdot 10^{-2}$ , 2 1, 3  $1 \cdot 10^2$

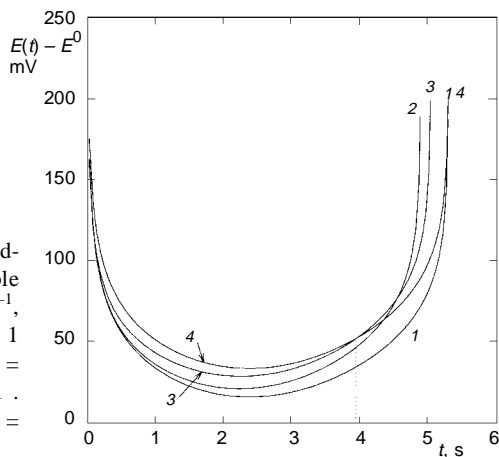


FIG. 3

Potential–time curves at a DME corresponding to an EC mechanism with a reversible charge transfer reaction;  $K = 1$ ,  $\omega = 0.8 \text{ s}^{-1}$ ,  $t_1 = 0.5 \text{ s}$ ,  $N_{\text{DME}} t_s^{2/3} = 2I_0 / nFA\omega\sqrt{D_A}C_A^* = 1 \text{ s}^{1/6}$ ,  $\xi_{\text{OA}} = \xi_{\text{OB}} = 0.15 \text{ s}^{-1/6}$ . The values of  $k = k_1 + k_2$  ( $\text{s}^{-1}$ ) are: 1  $1 \cdot 10^{-2}$ , 2 1, 3 10, 4  $1 \cdot 10^4$ . Vertical dotted line corresponds to  $t = \pi/\omega$ . Other conditions as in Fig. 2

above. The transition times corresponding to curves 2 and 3, calculated for intermediate  $k$  values are shorter. For  $\chi \geq 20$ , Eq. (27) is fulfilled and the  $E-t$  curves calculated at different values of  $k$  present a common point at  $t = \pi/\omega$ , independent on the chemical rate constants (curves 3 and 4 in Fig. 3). This common point can be used for determining the equilibrium constant when the chemical kinetic is rapid (Eq. (27)). This is shown in Fig. 4 where four types of curves with high values of the rate constants ( $k = 20, 50$  and  $100 \text{ s}^{-1}$ ) are plotted for different values of  $K$ . The potential corresponding to this point can be determined by setting  $X_B = 0$  and  $t = t_C = \pi/\omega$  in Eq. (22) for the EC process with a reversible electrochemical step. For example, for  $\gamma = 1$  and an SMDE with  $r_0 = 0.03 \text{ cm}$ ,  $D_A = 10^{-5} \text{ cm}^2 \text{ s}^{-1}$ ,  $\omega = 1 \text{ s}^{-1}$  and  $k = k_1 + k_2 = 10 \text{ s}^{-1}$  we obtain

$$E(t = \pi) = E^0 + \frac{RT}{nF} \ln \frac{1 + K}{0.017K} + \frac{RT}{nF} \ln \frac{2.410 - N_{\text{SMDE}}}{N_{\text{SMDE}}}, \quad (35)$$

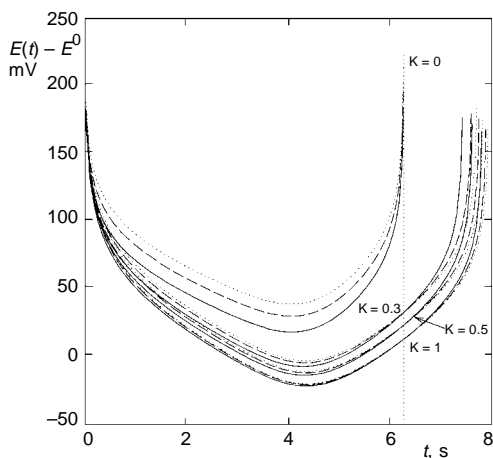


FIG. 4

Potential-time curves at an SMDE corresponding to an EC mechanism with a fast chemical reaction and a reversible charge transfer reaction,  $\omega = 0.5 \text{ s}^{-1}$ ,  $N_{\text{SMDE}} = 1 \text{ s}^{-1/2}$ ,  $\xi_{\text{SOA}} = \xi_{\text{SOB}} = 0.2 \text{ s}^{-1/2}$ . The curves are labelled with values of  $K$ . The values of  $k = k_1 + k_2$  ( $\text{s}^{-1}$ ) are: (—) 20, (---) 50, (···) 100. Vertical dotted line corresponds to  $t = \pi/\omega$ . Other conditions as in Fig. 2

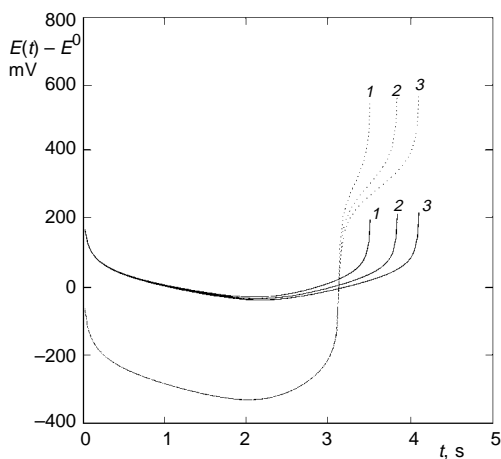


FIG. 5

Chemical and electrochemical reversibility effects on the potential-time curves corresponding to an EC mechanism at a SMDE;  $\omega = 1 \text{ s}^{-1}$ ,  $k = k_1 + k_2 = 1 \text{ s}^{-1}$ ,  $D_A = 10^{-5} \text{ cm}^2 \text{ s}^{-1}$ ,  $N_{\text{SMDE}} = 1.2 \text{ s}^{-1/2}$ ,  $\xi_{\text{SOA}} = \xi_{\text{SOB}} = 0.1 \text{ s}^{-1/2}$ ,  $\alpha = 0.5$ . The values of  $k_s$  ( $\text{cm s}^{-1}$ ) are: (—)  $1 \cdot 10^{-2}$ , (---)  $1 \cdot 10^{-5}$ . The values of  $K$  are: 1, 3, 100. Other conditions as in Fig. 2

where  $N_{\text{SMDE}}$  is given by Eq. (A17). From Eq. (35) with given value of  $N_{\text{SMDE}}$  value of  $K$  can be determined. Note that for  $K = 0$ ,  $t_c$  corresponds to the transition time.

Figure 5 shows the influence of the chemical equilibrium constant on  $E-t$  curves of an EC mechanism ( $k = 1 \text{ s}^{-1}$ ) with quasireversible (solid lines) or irreversible (dotted lines) electrochemical step. It can be seen that the influence of  $K$  on each situation is very different: The quasireversible process is affected by  $K$  throughout the complete chronopotentiogram; the totally irreversible process is not affected by the chemical equilibrium in its response to the cathodic current ( $\Omega < \pi$ ), whereas the anodic region ( $\Omega > \pi$ ) is affected strongly. It is in agreement with Eqs (23) and (24). Moreover, in the latter case, for  $K \rightarrow 0$  the decrease of  $\tau_B$  leads to the disappearance of characteristic shoulder of these curves, when the electrochemical step is irreversible<sup>7</sup>.

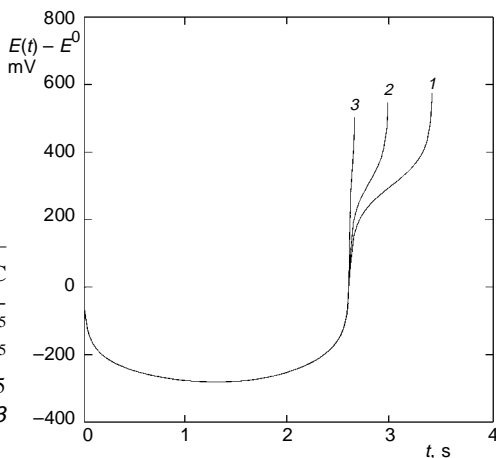


FIG. 6

Chemical rate constant effects on the potential-time curves at a DME corresponding to an EC mechanism when both chemical and electrochemical steps are irreversible;  $K = 0$ ,  $k_s = 1 \cdot 10^{-5} \text{ cm s}^{-1}$ ,  $\alpha = 0.5$ ,  $\omega = 1.2 \text{ s}^{-1}$ ,  $t_1 = 1 \text{ s}$ ,  $D_A = 1 \cdot 10^{-5} \text{ cm}^2 \text{ s}^{-1}$ ,  $N_{\text{DME}} t_S^{2/3} = 2I_0/nFA_0\sqrt{D_A}C_A^* = 1.5 \text{ s}^{1/6}$ . The values of  $k_1(\text{s}^{-1})$  are: 1 0.1, 2 1, 3 10. Other conditions as in Fig. 2

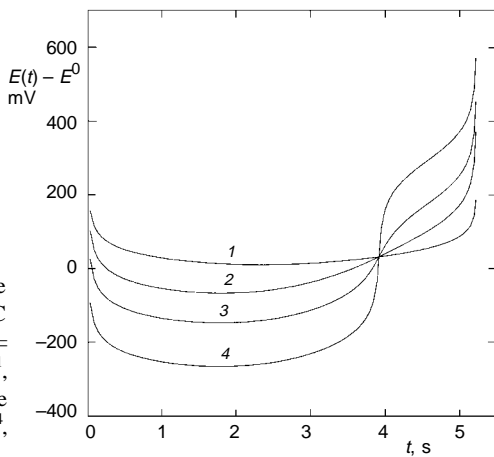


FIG. 7

Heterogeneous rate constant effects on the potential-time curves corresponding to an EC mechanism at a DME.  $K = 5$ ,  $k = k_1 + k_2 = 1.5 \text{ s}^{-1}$ ,  $\omega = 0.8 \text{ s}^{-1}$ ,  $t_1 = 0.5 \text{ s}$ ,  $D_A = 1 \cdot 10^{-5} \text{ cm}^2 \text{ s}^{-1}$ ,  $N_{\text{DME}} t_S^{2/3} = 2I_0/nFA_0\sqrt{D_A}C_A^* = 1.2 \text{ s}^{1/6}$ . The values of  $k_s(\text{cm s}^{-1})$  are: 1  $1 \cdot 10^3$ , 2  $2.5 \cdot 10^4$ , 3  $3.1 \cdot 10^4$ , 4  $4.1 \cdot 10^5$ . Other conditions as in Fig. 2

Figure 6 shows the effect of the homogeneous rate constant  $k_1$  on the  $E-t$  curves for an irreversible electrochemical process ( $k_s = 10^{-5} \text{ cm s}^{-1}$ ) and for an irreversible chemical reaction ( $K = 0$ ). In this case, the decrease of  $\tau_B$  due to the increase of  $k_1$ , yielded less enhanced shoulder. So, for high values of  $k_1$  the shoulder completely disappears (see curve 3 in Fig. 6).

We now shall analyze the influence of the reversibility of the electrochemical step on  $E-t$  curves. Figure 7 shows the influence of  $k_s$  on the EC mechanism for  $K = 5$ . The cathodic and anodic branches become more separated as  $k_s$  diminishes. For a totally irreversible process a shoulder appears on these curves. Furthermore, it can be seen that the point of intersection, whose ordinate corresponds to the polarographic crossing-potential, is independent on the heterogeneous kinetic parameters<sup>7-9</sup>.

#### *Determination of the Kinetic Parameters $\alpha$ and $k_s$ of the Electrochemical Step*

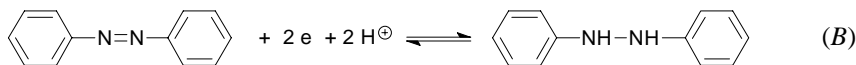
Electrochemical kinetic parameters can be obtained by linear regression analysis of  $E(t)$  vs  $\ln(g_C)$  and  $E(t)$  vs  $\ln(g_A)$  plots in agreement with Eqs (23) and (24). Thus, it is possible to discriminate between an EC and an E process, since in the latter case the function  $g_C$  is identical to that obtained for an EC mechanism, while the function  $g_A$  has a different form.

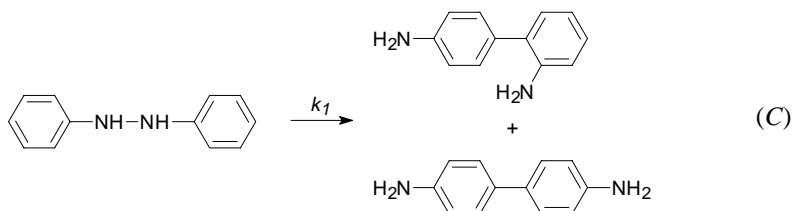
### EXPERIMENTAL

Waveforms generation and data acquisition were performed using i-SBXDDA4 and DAS16-330i (ComputerBoards, U.S.A.) boards, respectively. All computer programs were written in our laboratory. Computer driven potentiostat-galvanostat was designed and constructed by QUICELTRON (Spain). A SMDE was constructed using a DME, EA 1019-1 (Metrohm) to which a home-made valve was sealed. Different open times in this valve allowed electrode radii to be between 0.01 and 0.05 cm. A reference was Ag/AgCl/KCl(sat) electrode. Working solutions (40% (v/v) ethanol) were prepared from an ethanolic  $10 \text{ mmol l}^{-1}$  azobenzene stock solution (stored in dark) to which appropriate amounts of water, ethanol and aqueous solutions of  $\text{HClO}_4$  and  $\text{NaClO}_4$  were added. In all experiments the temperature was kept constant at  $25 \pm 0.2 \text{ }^\circ\text{C}$ . Other methods and experimental conditions are described in ref.<sup>7</sup>.

### EXPERIMENTAL RESULTS

To verify methods proposed in this paper for the determination of the kinetic parameters of the chemical step, the well known reduction of azobenzene was used according to Eqs (B), (C).





Here, azobenzene is reduced to hydrazobenzene which undergoes benzidine rearrangement in strong acid. The kinetic studies reported<sup>10,11</sup> show that the rearrangement is of the first order for hydrazobenzene and of the second order for hydronium ions. According to these studies, in the presence of a strong acid, the process is of pseudo first order in hydrazobenzene, and the charge transfer reaction is reversible.

Figure 8 shows alternating current chronopotentiograms of azobenzene at several acid concentrations. The theoretical transition time  $\tau_{B_E}$  of species B corresponding to an electrochemical process is shown in this figure. As discussed above,  $\tau_{B_E}$  is an upper limit for  $\tau_B$ . Apparently, this figure shows the presence of a chemical reaction (influenced by acid concentration) following the charge transfer reaction. We can also see the complication appearing in the reduction mechanism of azobenzene in an unbuffered neutral medium (curve 1). The appearance of the shoulder associated with a quasireversible charge transfer reaction is evident. Due to more complex interpretation of azobenzene reduction in a neutral medium, no kinetic analysis was carried out for this case.

An interesting problem is the measurement of transition times. In fact, each proposed method implies some degree of arbitrariness. We have measured  $\tau_B$  as the point at which the concavity of the suddenly ascendant  $E-t$  curve changes. For this purpose, the first derivative of the  $E-t$  curve was calculated and the transition time was defined by the point at which the derivative reached its maximum value, as illustrated in Fig. 9.

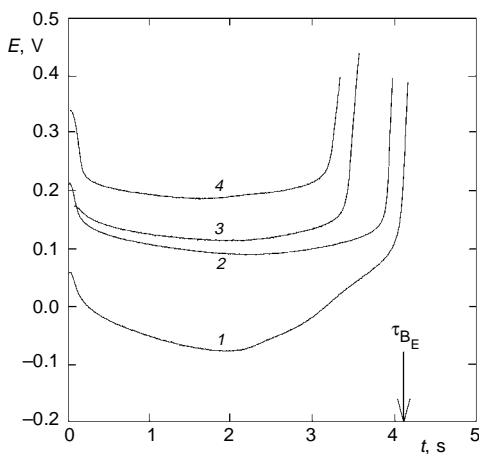


FIG. 8

Experimental potential-time curves at an SMDE corresponding to  $2 \text{ mmol l}^{-1}$  azobenzene;  $\omega = 1 \text{ s}^{-1}$ ,  $I_0 = 3.5 \text{ }\mu\text{A}$ ,  $r_0 = 0.026 \text{ cm}$ . The concentrations of  $\text{HClO}_4$  and  $\text{NaClO}_4$  (in  $\text{mol l}^{-1}$ ) are as follows: 1 0, 1.5; 2 0.25, 1.25; 3 0.63, 0.87; 4 1.25, 0.25

According to Eq. (19)  $\tau_B$  is independent of  $I_0$  for an EC process. In Fig. 10 we can see this independence for benzidine rearrangement. Moreover, this characteristic is assumed as a diagnosis for the absence of a double layer capacitive distortion, since when capacitive effects are present,  $\tau_B$  is dependent on  $I_0$  (ref.<sup>16</sup>).

The results of our kinetic analysis carried out at three acid concentrations are shown in Table I. As pointed out, for the calculation of the chemical rate constants it is necessary to assume a value for  $K$  (the chemical equilibrium constant). According to previous reports<sup>10-14</sup>, we assume  $K = 0$ . As shown in Table I, the values found for the rate constant are practically independent of  $\omega$ , indicating a good performance of the method and also that the assumption of  $K = 0$  is correct (hence  $k_1 \gg k_2$ ). A direct comparison of our results with those previously given in the literature is not immediate, because these studies have been carried out under a wide range of experimental condi-

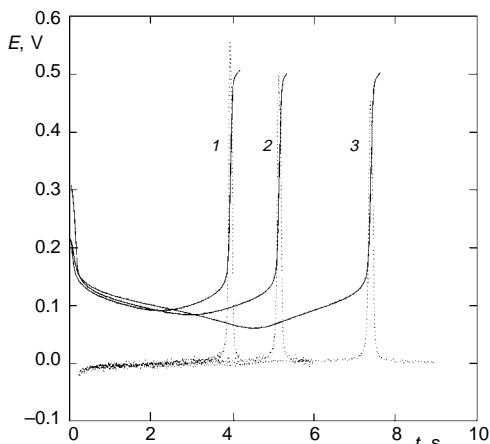


FIG. 9

Experimental potential-time curves at an SMDE (solid lines) and their first derivative (dashed lines) corresponding to 2 mmol  $\Gamma^{-1}$  azobenzene in 0.25 mol  $\Gamma^{-1}$  HClO<sub>4</sub> and 1.25 mol  $\Gamma^{-1}$  NaClO<sub>4</sub>;  $I_0 = 3.5 \mu\text{A}$ ,  $r_0 = 0.026 \text{ cm}$ . The values of  $\omega$  ( $\text{s}^{-1}$ ) are: 1 1.00, 2 0.75, 3 0.50

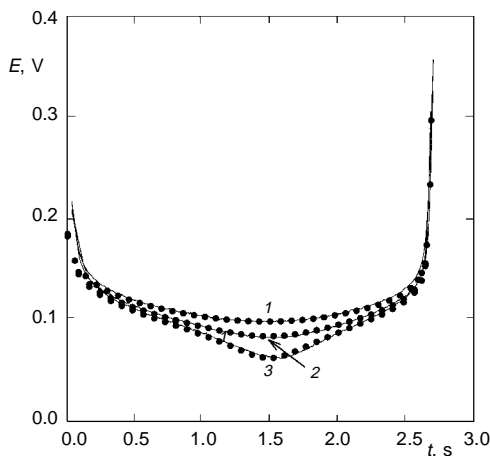


FIG. 10

Experimental potential-time curves at an SMDE (solid lines) corresponding to 2 mmol  $\Gamma^{-1}$  azobenzene in 0.25 mol  $\Gamma^{-1}$  HClO<sub>4</sub> and 1.25 mol  $\Gamma^{-1}$  NaClO<sub>4</sub>;  $\omega = 1.5 \text{ s}^{-1}$ ,  $r_0 = 0.026 \text{ cm}$ . The values of  $I_0$  ( $\mu\text{A}$ ) are: 1 3.5, 2 5, 3 6. Circles correspond to theoretical curves calculated for a reversible charge transfer reaction with  $K = 0$ ,  $\omega = 1.5 \text{ s}^{-1}$ ,  $\xi_{0A} = \xi_{0B} = 0.138 \text{ s}^{-1/2}$ ,  $\mu_{\text{EC}} = 0$ ,  $\gamma = 1$ ,  $T = 298 \text{ K}$ ,  $E^0 = 0.100 \text{ V}$ . The values of  $N_{\text{SMDE}}$  ( $\text{s}^{-1/2}$ ) are: 1 1.193, 2 1.705, 3 2.046

TABLE I

Kinetic data for the perchloric acid-catalyzed rearrangement of hydrazobenzene in 40% (v/v) ethanol-water solution of  $\text{HClO}_4 + \text{NaClO}_4$  mixture at 25 °C. Azobenzene  $2 \text{ mmol l}^{-1}$ ,  $r_0 = 0.026 \text{ cm}$ . It is assumed that  $D_A = D_B = 3.2 \cdot 10^{-6} \text{ cm}^2 \text{ s}^{-1}$  (A = azobenzene, B = hydrazobenzene)

$\omega, \text{ s}^{-1}$	$I_0, \mu\text{A}$	$\tau_B, \text{ s}$	$k_i, \text{ s}^{-1}$
$[\text{HClO}_4] = 0.25 \text{ mol l}^{-1}, [\text{NaClO}_4] = 1.25 \text{ mol l}^{-1}$			
0.5	3.5	7.55	0.16
0.75	3.5	5.16	0.16
1.0	5.0	3.94	0.14
1.5	6.0	2.65	0.18
2.0	6.0	2.02	0.13
3.0	7.5	1.36	0.13
4.0	10.0	1.02	0.19
mean value: $0.15 \pm 0.02$			
$[\text{HClO}_4] = 0.63 \text{ mol l}^{-1}, [\text{NaClO}_4] = 0.87 \text{ mol l}^{-1}$			
0.5	3.5	6.68	1.15
0.75	3.5	4.52	1.30
1.0	5.0	3.44	1.38
1.5	6.0	2.36	1.39
2.0	6.0	1.82	1.28
3.0	7.5	1.25	1.26
4.0	10.0	0.96	1.16
mean value: $1.27 \pm 0.09$			
$[\text{HClO}_4] = 1.25 \text{ mol l}^{-1}, [\text{NaClO}_4] = 0.25 \text{ mol l}^{-1}$			
0.5	5.0	6.43	3.26
0.75	7.5	4.33	3.36
1.0	7.5	3.28	3.39
1.5	7.5	2.22	3.65
2.0	7.5	1.69	3.73
3.0	7.5	1.16	3.60
4.0	10.0	0.89	3.53
mean value: $3.50 \pm 0.17$			

tions. However, consulting refs<sup>10-14</sup>, the agreement with our results is clearly seen. For example, in ref.<sup>11</sup>, for a composition of solution similar to our own, 40% (v/v) ethanol and 0.25 mol l<sup>-1</sup> HClO<sub>4</sub>, they obtained a value for  $k_1 = 0.143 \text{ s}^{-1}$ , while the value obtained by us under analogous conditions (except of the concentration of NaClO<sub>4</sub>) was  $k_1 = 0.15 \text{ s}^{-1}$ .

## CONCLUSIONS

The application of an alternating current to spherical electrodes is a very powerful technique for characterizing an EC mechanism, under conditions at which the transition time of the oxidized species  $\tau_A$  is not reached. Under these conditions, the transition time of the reduced species  $\tau_B$  is always reached during the first cycle of the alternating current if species B is not initially present in solution. It involves an important homogeneous kinetic information and does not depend on most experimental details such as the alternating current amplitude  $I_0$ , the electrode area and the initial concentration of the oxidized species. A suitable time scale for each kinetic situation is achieved by selecting an appropriate value of  $\omega$ .

The EC mechanism behaves as an E mechanism in the two cases:  $\chi \rightarrow 0$ ,  $K > 0$  and  $K \gg 1$ , any value of  $\chi$ .

When  $K = 0$  the EC mechanism shows the most pronounced kinetic character according to Eq. (29). In this case, the oxidation transition time,  $\tau_B$ , diminishes when the homogeneous rate constant  $k_1$  increases. When  $K > 0$ ,  $\tau_B$  diminishes initially with  $k_1 + k_2$  until it reaches its minimum value. Then  $\tau_B$  increases to its upper limit given by the oxidation transition time of an E process  $\tau_{B_E}$ .

For totally irreversible charge transfer reaction, the cathodic region of  $E-t$  curves is identical for both E and EC mechanisms, while the anodic region is strongly dependent on homogeneous kinetics.

The procedures described in this paper for calculating chemical rate constants have been applied to the benzidine rearrangement reaction. The values obtained are in agreement with previous studies<sup>10-14</sup>.

## APPENDIX

The series  $S_i$  ( $i = A$  or  $B$ ) and  $X_B$  in the expressions for surface concentrations depend on the type of the electrode. In this work these series have been derived for the DME because for this electrode the problem is more general. Moreover, expressions derived for the expanding sphere electrode can be simply transformed for static spherical electrode (SMDE) and for planar electrode (PE).

The  $S_i$  and  $X_B$  series for a DME are given by

$$S_i = S_i(\xi, \beta, \Omega) = \sum_{n=0}^{\infty} \frac{(-1)^n \Omega^{2n+1}}{(2n+1)!} G_n(\xi, \beta) \quad (A1)$$



$$G_n(\xi_i, \beta) = G_n^{(0)}(\beta) - \xi_i G_n^{(1)}(\beta) + \xi_i^2 G_n^{(2)}(\beta) + \dots \quad (A2)$$

$$G_n^{(0)}(\beta) = \frac{1}{P_{4n+3}} \left\{ 1 + \frac{\beta^3}{3(4n+5)} + \frac{7}{18} \frac{\beta^6}{(4n+5)(4n+7)} + \right. \\ \left. + \frac{20}{27} \frac{\beta^9}{(4n+5)(4n+7)(4n+9)} + \dots \right\} \quad (A3)$$

$$G_n^{(1)}(\beta) = \frac{1}{4(2n+2)} + \frac{\beta^3}{8(2n+2)(2n+3)} + 3 \frac{\beta^6}{32(2n+2)(2n+3)(2n+4)} + \dots \quad (A4)$$

$$G_n^{(2)}(\beta) = \frac{1}{P_{4n+3}} \left\{ \frac{1}{2(4n+5)} + \frac{\beta^3}{(4n+5)(4n+7)} + \dots \right\}, \quad (A5)$$

where  $\Omega$ ,  $\xi_i$  and  $\beta$  are dimensionless parameters given by

$$\Omega = \omega t \quad (A6)$$

$$\beta = \frac{t}{t_1 + t} = \frac{\Omega}{\Omega_1 + \Omega} \quad (A7)$$

with

$$\Omega_1 = \omega t_1 \quad (A8)$$

$$\xi_i = \frac{2(D_i t)^{1/2}}{r_0} \quad (A9)$$

$$X_B = X_B(\xi_B, \beta, \chi, \Omega) = \exp(-\chi) \sum_{j,n}^{\infty} \frac{(-1)^n \Omega^{2n+1} \chi^j}{(2n+1)! j!} J_{j,n}(\xi_B, \beta) \left. \right\} \quad (A10)$$

$$J_{j,n}(\xi_B, \beta) = J_{j,n}^{(0)}(\beta) - \xi_B J_{j,n}^{(1)}(\beta) + \xi_B^2 J_{j,n}^{(2)}(\beta)$$

$$J_{j,n}^{(0)}(\beta) = \frac{1}{P_{2j+4n+3}} \left\{ 1 + \frac{\beta^3}{3(2j+4n+5)} + \frac{7}{18} \frac{\beta^6}{(2j+4n+5)(2j+4n+7)} + \right. \\ \left. + \frac{20}{27} \frac{\beta^9}{(2j+4n+5)(2j+4n+7)(2j+4n+9)} + \dots \right\} \quad (A11)$$

$$J_{j,n}^{(1)}(\beta) = \frac{1}{4(j+2n+2)} + \frac{\beta^3}{8(j+2n+2)(j+2n+3)} +$$

$$+ \frac{3\beta^6}{32(j+2n+2)(j+2n+3)(j+2n+4)} + \dots \quad (A12)$$

$$J_{j,n}^{(2)}(\beta) = \frac{1}{P_{2j+4n+3}} \left\{ \frac{1}{2(2j+4n+5)} + \frac{\beta^3}{(2j+4n+5)(2j+4n+7)} + \dots \right\} \quad (A13)$$

$$\chi = kt \quad (A14)$$

### Particular Cases

*Null blank period* ( $t_1 = 0$ ). In this case the alternating current given by Eq. (10) is applied from the beginning of the drop life and Eqs (A1)–(A5) can be included in Eqs (11)–(12) by setting  $\beta = 1$ .

*Stationary spherical electrode.* Equations (11) and (12) for  $C_A(r_0, t)$  and  $C_B(r_0, t)$  can be transformed for a stationary electrode of area  $A = A_0 = A_0 t_1^{2/3}$  by assuming  $t_1 \gg t$  (or  $\beta = 0$ ) in Eqs (A3)–(A5), (A11)–(A13). Thus,

$$\frac{C_A(r_0, t)}{C_A^*} = 1 - N_{\text{SMDE}} t^{1/2} S_{\text{A,SMDE}} \quad (A15)$$

$$\frac{C_B(r_0, t)}{C_A^*} = \frac{1}{1+K} \left\{ K\mu_{\text{EC}} + \gamma N_{\text{SMDE}} t^{1/2} \left[ K S_{\text{B,SMDE}} + X_{\text{B,SMDE}} \right] \right\} \quad (A16)$$

$$N_{\text{SMDE}} = \frac{2I_0}{nFA\sqrt{D_A} C_A^*} \quad (A17)$$

$$S_{i,\text{SMDE}} = \sum_{n=0}^{\infty} \frac{(-1)^n \Omega^{2n+1}}{(2n+1)!} \left[ \frac{1}{P_{4n+3}} - \frac{1}{4(2n+2)} \xi_i + \frac{1}{2(4n+5)P_{4n+3}} \xi_i^2 + \dots \right] \quad (A18)$$

$$X_{\text{B,SMDE}} = \exp(-\chi) \sum_{j,n} \frac{(-1)^n \Omega^{2n+1}}{(2n+1)! j!} \chi^j \left[ \frac{1}{P_{2j+4n+3}} - \frac{1}{4(j+2n+2)} \xi_i + \right.$$

$$\left. + \frac{1}{2P_{2j+4n+3}} \frac{1}{(2j+4n+5)} \xi_i^2 + \dots \right] \quad (A19)$$

*Stationary plane electrode.* Equations (11) and (12) are transformed for a stationary plane electrode of area  $A = A_0 t_1^{2/3}$  by setting  $\xi_i = 0$  and  $\beta = 0$ .

### SYMBOLS

$a$	$(3m_{\text{Hg}}/4\pi d)^{1/3}$
$A(t_s)$	time dependent electrode area for a DME ( $= A_0 t_s^{2/3}$ )
$A_0$	electrode area at $t_s = 1$ s ( $A_0 = (4\pi)^{1/3}(3m_{\text{Hg}}/d)^{2/3}$ )
$D_i$	diffusion coefficient of species $i$ , $i = A, B$ or $C$
$E^0$	formal standard potential of the electroactive couple
$k$	$k_1 + k_2$
$k_1, k_2$	homogeneous rate constants of the forward and reverse first order chemical reaction
$k_S$	heterogeneous rate constant of charge transfer at $E^0$
$K$	$C_B^*/C_C^*$
$m_{\text{Hg}}, d$	rate of flow and density of mercury
$P_j$	$2\Gamma(1 + j/2)/\Gamma[(1 + j)/2]$
$r_0$	electrode radius at time $t_s$ for a DME ( $r_0 = a t_s^{1/3}$ ) or fixed electrode radius for an SMDE
$t$	time elapsed between the application of the alternating current and the measurement of the potential
$t_S$	$t_1 + t$
$t_1$	blank period used, optionally, only with DME
$\beta$	$t/(t + t_1) = \Omega/(\Omega + \Omega_1)$
$\Gamma$	Euler Gamma function
$\mu_{\text{EC}}$	$(C_B^* + C_C^*)/C_A^*$
$\xi_i$	$2\sqrt{D_i t}/r_0$
$\xi_{0i}$	$\xi_i/\sqrt{t}$ for an SMDE, $\xi_i t_s^{1/3}/\sqrt{t}$ for a DME
$\tau_A$	reduction transition time for an EC process
$\tau_B$	oxidation transition time for an EC process
$\tau_{BE}$	oxidation transition time corresponding to an E process
$\chi$	$kt$
$\omega$	angular frequency of alternating current ( $2\pi f$ , where $f$ is conventional frequency in Hz)
$\Omega$	$\omega t$
$\Omega_1$	$\omega t_1$

Other symbols have their usual meaning.

*The authors greatly appreciate the financial support from the Direccion General de Investigacion Cientifica y Tecnica (project No. PB93-1134) and to the DREUCA de la Region de Murcia (project No. PIB94/73). We also acknowledge the critical reading of this manuscript by Dr M. L. Alcaraz. We would also like to express our gratitude to the reviewer, who has greatly helped us to improve this paper with his valuable suggestions.*

### REFERENCES

1. Molina A., Lopez-Tenes M.: Collect. Czech. Chem. Commun. 56, 1 (1991).
2. Dracka O.: Collect. Czech. Chem. Commun. 25, 338 (1958).
3. Fischer O., Dracka O.: J. Electroanal. Chem. 75, 301 (1977).
4. Herman H. B., Bard A. J.: Anal. Chem. 35, 1121 (1963).

5. McDonald D. D.: *Transient Techniques in Electrochemistry*, Chap. 5. Plenum, New York 1977.
6. Bard A. J., Faulkner L. R.: *Electrochemical Methods*, Chap 7 and 11. Wiley, New York 1980.
7. Martinez-Ortiz F., Molina A., Serna C.: *J. Electroanal. Chem.* 308, 97 (1991).
8. Molina A., Martinez-Ortiz F., Serna C.: *J. Electroanal. Chem.* 336, 1 (1992).
9. Molina A., Ruiz R., Martinez-Ortiz F., Lopez-Tenes M.: *Collect. Czech. Chem. Commun.* 61, 973 (1996).
10. Schwarz W. M., Shain I.: *J. Phys. Chem.* 69, 30 (1965).
11. Oglesby D. M., Johnson J. D., Reilley C. N.: *Anal. Chem.* 38, 385 (1966).
12. Schwarz W. M., Shain I.: *J. Phys. Chem.* 70, 845 (1966).
13. Lundquist J. T., Nicholson R. S.: *J. Electroanal. Chem.* 16, 445 (1968).
14. Kim M. H.: *Anal. Chem.* 59, 2136 (1987).
15. Heyrovsky J., Kuta J.: *Principles of Polarography*, p. 92. Academic Press, New York 1966.
16. Martinez-Ortiz F., Molina A., Carceles C., Lopez-Tenes M.: Unpublished results.